

# Anisotropic Susceptibility of $\text{La}_{2-x}\text{Sr}_x\text{CoO}_4$ related to the Spin States of Cobalt

N Hollmann<sup>1</sup>, M W Haverkort<sup>1</sup>, M Cwik<sup>1</sup>, M Benomar<sup>1</sup>,  
M Reuther<sup>1</sup>, A Tanaka<sup>2</sup>, T Lorenz<sup>1</sup>

<sup>1</sup>II. Physikalisches Institut, University of Cologne, Zùlpicherstrasse 77, D-50937 Kùln, Germany

<sup>2</sup>Department of Quantum Matter, ADSM, Hiroshima University, Higashi-Hiroshima 739-8530, Japan

E-mail: hollmann@ph2.uni-koeln.de

## Abstract.

We present a study of the magnetic susceptibility of  $\text{La}_{2-x}\text{Sr}_x\text{CoO}_4$  single crystals in a doping range  $0.3 \leq x \leq 0.8$ . Our data shows a pronounced magnetic anisotropy for all compounds. This anisotropy is in agreement with a low-spin ground state ( $S = 0$ ) of  $\text{Co}^{3+}$  for  $x \geq 0.4$  and a high-spin ground state ( $S = 3/2$ ) of  $\text{Co}^{2+}$ . We compare our data with a crystal-field model calculation assuming local moments and find a good description of the magnetic behavior for  $x \geq 0.5$ . This includes the pronounced kinks observed in the inverse magnetic susceptibility, which result from the anisotropy and low-energy excited states of  $\text{Co}^{2+}$  and are not related to magnetic ordering or temperature-dependent spin-state transitions.

PACS numbers: 71.20.Be, 71.70.Ch, 71.70.Ej, 75.30.Gw

Transition-metal oxides are known for their complex interplay between different degrees of freedom like spin, charge and orbitals. In some of these systems another interesting property is found: ions like  $\text{Co}^{3+}$  in a crystal-field environment can occur in different spin states. Additionally, transitions between different spin states are possible for some compounds. A prominent example showing this phenomenon is  $\text{LaCoO}_3$ , which has been examined and discussed since the middle of the last century (see e.g. Refs. [1–11]).

The existence of different spin states arises from the competition between crystal-field effects and on-site Coulomb interaction. Crystal fields lift the degeneracy of the  $3d$  states. If the crystal field is strong, this can lead to a violation of Hund's rules. In the case of cubic symmetry and in a one-electron picture, the five-fold degenerate  $3d$  states are split into a three-fold degenerate  $t_{2g}$  and a two-fold degenerate  $e_g$  level. The splitting between  $t_{2g}$  and  $e_g$  states is called  $10Dq$ . With a strong crystal field, the electrons will be forced into the low-spin state (LS). Regarding a  $3d^6$  system, this state consists of an antiparallel alignment of spins with  $t_{2g}^6 e_g^0$  and  $S = 0$ . On the other hand, the Coulomb interaction manifests itself in the effect of Hund's coupling. A parallel arrangement of spins minimizes the electron-electron repulsion because the Pauli principle forces the electrons to occupy different orbitals. In a weak cubic crystal field, this effect will dominate and lead to the high-spin state (HS), which is the configuration with the highest total spin possible in accordance with the Pauli principle. For a  $3d^6$  system, this configuration is  $t_{2g}^4 e_g^2$  with  $S = 2$ . For  $\text{Co}^{3+}$  the crossover between these two different spin states occurs roughly at an energy difference of  $10Dq = 2.2\text{eV}$ .

In the case of  $\text{LaCoO}_3$ , a low-spin ground state for  $\text{Co}^{3+}$  was found [2]. Interestingly, the difference between the crystal field energies and the promotional energies is so small that an excited state with different spin state can be reached by thermal excitation. This excited state has been a subject of debate for a long time. Apart from the HS state described above, the intermediate-spin state (IS,  $t_{2g}^5 e_g^1$   $S = 1$ ) was also discussed [4] and reported in many experiments, but it was shown that it might have been confused with a spin-orbit coupled HS state [11].

For the layered cobaltates  $\text{La}_{2-x}\text{Sr}_x\text{CoO}_4$ , much less is known about the spin state of  $\text{Co}^{3+}$ . Based on magnetic measurements [12] a HS ground state for  $x \leq 0.7$  and a spin-state transition to an IS ground state for  $x > 0.7$  was proposed. This conclusion was based on a Curie-Weiss analysis of the susceptibility in a temperature range of 100K to 300K and NMR measurements [13]. Unrestricted Hartree-Fock calculations [14] showed a slightly different picture. Here, three different magnetic phases were found. An antiferromagnetic HS phase ( $x < 0.39$ ), a ferromagnetic HS phase ( $0.39 \leq x \leq 0.52$ ) and an antiferromagnetic LS-HS-ordered phase ( $x > 0.52$ ) were proposed. These calculations were also based on the results of the Curie-Weiss analysis in Ref. [12]. Taking into account that  $\text{La}_{2-x}\text{Sr}_x\text{CoO}_4$  is an anisotropic material with rather strong spin-orbit coupling compared to the tetragonal crystal field splitting, the validity of the Curie-Weiss law is questionable. The aim of this paper is to analyze the magnetic susceptibility from a different perspective, concentrating on the spin state of  $\text{Co}^{3+}$ .

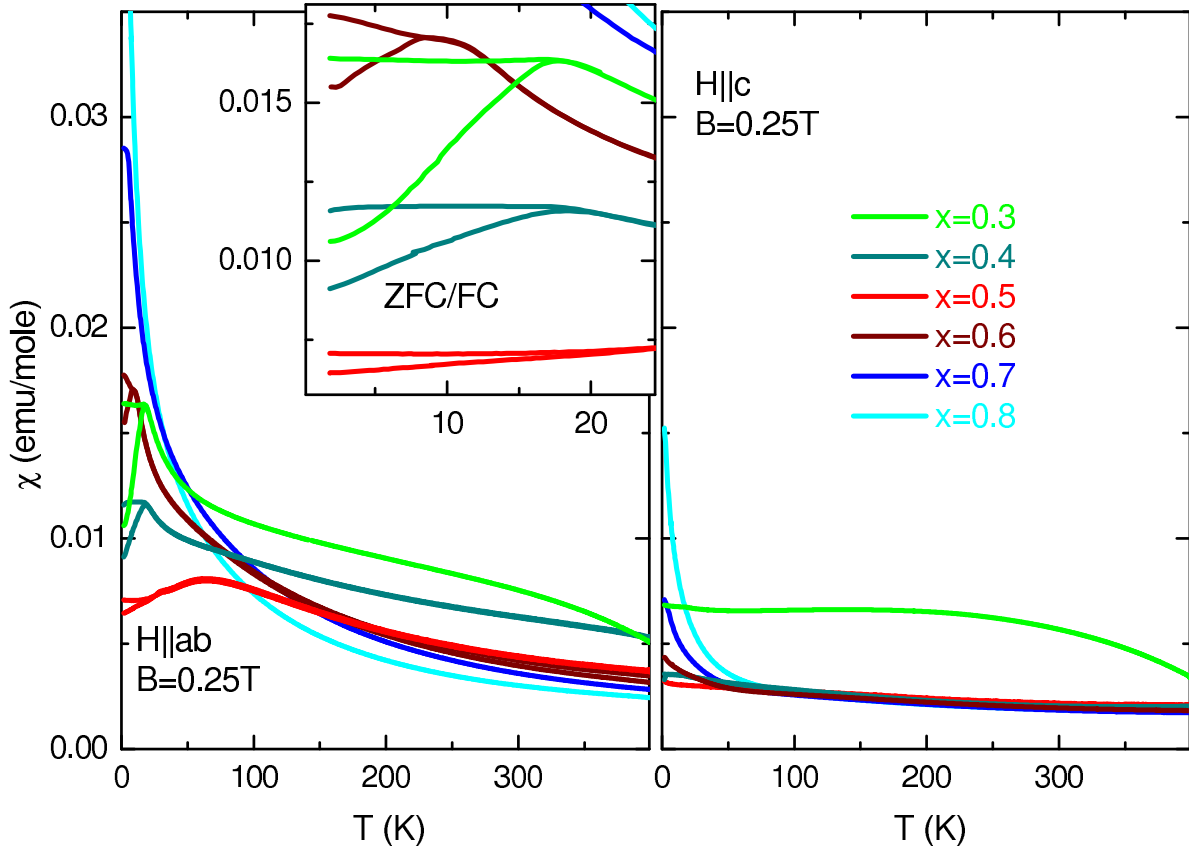


Figure 1: Magnetic susceptibility of  $\text{La}_{2-x}\text{Sr}_x\text{CoO}_4$  for two different directions of the magnetic field. The insert is an expanded view of the low-temperature region to show the difference between FC and ZFC measurements for  $0.3 \leq x \leq 0.6$ . The curves with the lower susceptibility refer to the ZFC measurements.

The single crystals used for the magnetic measurements have been grown using the floating-zone technique in an image furnace. A strontium doping range of  $0.3 \leq x \leq 0.8$  was covered. Resistivity measurements revealed that  $\text{La}_{2-x}\text{Sr}_x\text{CoO}_4$  is a strong insulator for all Sr doping concentrations. The  $x = 0.5$  sample turned out to possess the highest resistivity, which is in accordance with the charge ordering of  $\text{Co}^{2+}$  and  $\text{Co}^{3+}$  at  $\approx 750\text{K}$  that has already been reported [15].

The magnetization was measured with a Quantum Design vibrating sample magnetometer (VSM). The field was aligned parallel to the  $\text{CoO}_2$  planes as well as perpendicular to these planes (the crystallographic  $c$  direction). The corresponding components  $\chi_{ab}$  and  $\chi_c$  are plotted in Fig. 1. A short-range antiferromagnetic order has been found in the compounds  $0.3 \leq x \leq 0.6$  by neutron measurements [16]. This frustrated short-range order is also reflected by the difference between field cooled (FC) and zero-field cooled (ZFC) measurements at low temperatures. The susceptibility is smaller for ZFC than FC below a certain freezing temperature.

Figure 2 shows the inverse magnetic susceptibility for both orientations of field. The main feature of the susceptibility in the paramagnetic regime is the pronounced

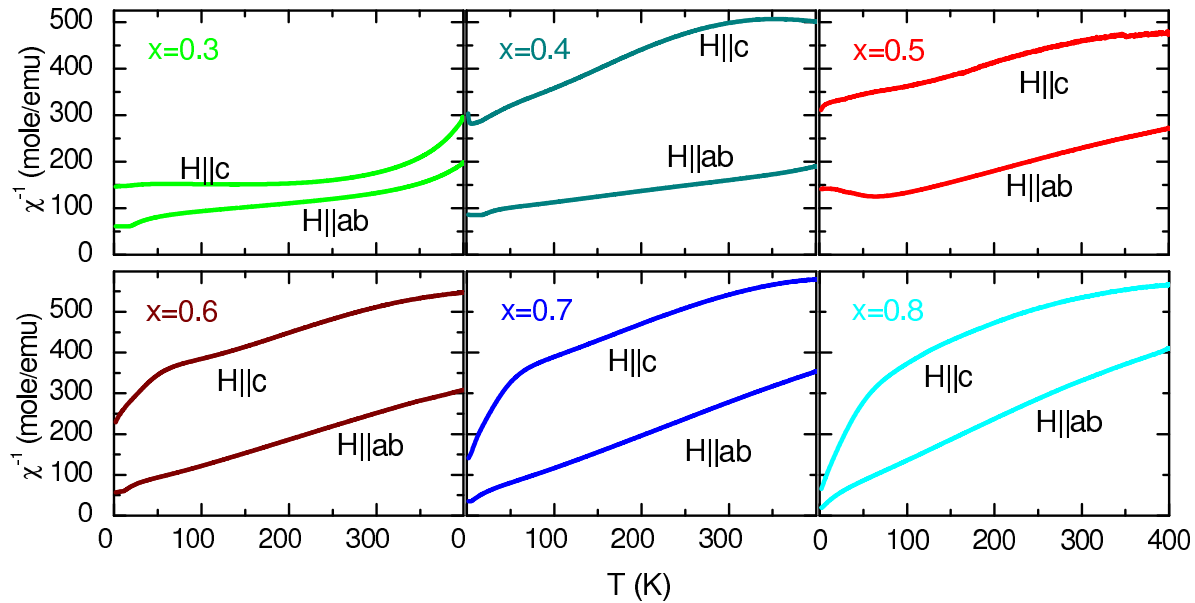


Figure 2: Inverse susceptibility of  $\text{La}_{2-x}\text{Sr}_x\text{CoO}_4$  for two different directions of the magnetic field. The form of the curves and the magnetic anisotropy strongly deviates from Curie-Weiss behavior.

magnetic anisotropy, both in magnitude and form of the curves. The direction of the anisotropy is the same for all crystals, finding  $\chi_{ab}$  to be bigger than  $\chi_c$ .

Here, the magnetic anisotropy arises from band structure and spin-orbit coupling. For Mott and charge-transfer insulators with well-localized moments, band-structure and covalency effects can be approximated by an effective crystal field. The crystal field reflects the anisotropy of the lattice and lifts the degeneracy of the  $3d$  states, resulting in a new set of linear combinations of the unperturbed wave functions as a basis. The expectation values of the components of the orbital moment result from these new linear combinations. Thus, the crystal's anisotropy may result in an anisotropy of the orbital moment. Spin-orbit coupling ties the spin moment to this anisotropy. The spin-orbit coupling Hamiltonian will be written as  $\zeta \sum_i l_i \cdot s_i$  where the sum over  $i$  runs over all electrons. The dot product between spin and orbital momentum tends to align these moments antiparallel for each electron. For an anisotropic orbital momentum, the spin is aligned in the direction of maximum orbital momentum [17].

The full many-body ground-state for a  $d^6$  or  $d^7$  configuration in a crystal-field calculation including spin-orbit coupling and a tetragonal distortions is not simple [18] but well known. In order to get an intuitive picture one would like to fall back to a single electron description. In the limit of full spin polarization this can be done and gives important results. In the following we will first discuss the magnetic anisotropy of  $\text{La}_{2-x}\text{Sr}_x\text{CoO}_4$  in terms of a one-electron picture. We will show that each spin state has a different magnetic anisotropy from which, by comparison to the experiment, the spin states of the Co ion can be concluded. In order to obtain also a quantitative description and to verify our simple argumentation we will present a full many-body crystal-field

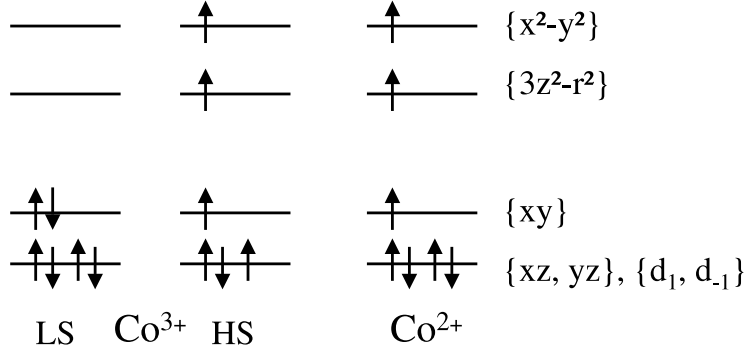


Figure 3: Splitting of the  $3d$  levels in a tetragonal crystal field arising from an elongated oxygen octahedron. The two sketches on the left show the occupation for the LS and HS state of  $\text{Co}^{3+}$  in a one-electron picture. The right sketch refers to HS  $\text{Co}^{2+}$ . The real orbitals on the right can be used as a basis.

calculation afterwards.

Within a cubic crystal structure, the  $3d$  states split into  $e_g$  orbitals and  $t_{2g}$  orbitals. The basis can be chosen as  $\{3z^2 - r^2, x^2 - y^2\}$  and  $\{xy, xz, yz\}$ , respectively. A partially filled  $t_{2g}$  shell can produce a pseudo orbital moment of  $\tilde{L} = 1$ . Though the individual real wave functions  $d_{xy}$ ,  $d_{yz}$  and  $d_{xz}$  of the basis themselves have a completely quenched orbital moment, their linear combinations are in general complex. Writing  $d_{m_l}^x$ ,  $d_{m_l}^y$  and  $d_{m_l}^z$  as the orbital wave function with the orbital moment quantized along the axes  $x$ ,  $y$  and  $z$ , respectively, one finds

$$d_{\pm 1}^x = \frac{1}{\sqrt{2}}(\pm d_{xy} + id_{xz}) \quad (1)$$

$$d_{\pm 1}^y = \frac{1}{\sqrt{2}}(\pm d_{yz} + id_{xy}) \quad (2)$$

$$d_{\pm 1}^z = \frac{1}{\sqrt{2}}(\pm d_{xz} + id_{yz}). \quad (3)$$

In the limit of very large crystal field splittings  $10Dq$  and with a partially filled  $t_{2g}$  shell, the moment is isotropic, despite the large orbital moment. In fact, the  $t_{2g}$  electrons are sometimes compared to  $p$  electrons [19].

Introducing a tetragonal distortion, the orbital moment becomes anisotropic. The tetragonal crystal field splits the cubic  $e_g$  states into non-degenerate  $a_{1g}$  and  $b_{1g}$  levels, while the  $t_{2g}$  states split into a non-degenerate  $b_{2g}$  state and a two-fold degenerate  $e_g$  level. As a basis for these states, the real orbital functions can also be used. The  $z$  axis of the system is taken to be identical with the  $c$  axis of the crystal. In the case of  $\text{La}_{2-x}\text{Sr}_x\text{CoO}_4$ , the oxygen octahedron is elongated in the  $c$  direction. The order of levels and occupations for the ground states of the two cobalt ions is illustrated in Fig. 3.

The  $\text{Co}^{3+}$  low-spin state is, except for a small Van Vleck susceptibility, nonmagnetic since it does not carry any moment. In the high-spin state,  $\text{Co}^{3+}$  has spin and orbital

moment. The orbital degeneracy is not completely quenched: the degenerate  $xz$  and  $yz$  are occupied by three electrons. These real orbitals can thus be recombined to form complex orbitals carrying orbital moment in the  $z$  direction as described in Eq. (3). Note that the linear combinations in equations (1) and (2) cannot be formed because the  $xy$  orbital is not degenerate with the  $xz$  and  $yz$  orbitals. Therefore the orbital moment is larger in the  $z$  direction making this the easy axis. This anisotropy should be reflected in the susceptibility with  $\chi_c > \chi_{ab}$ , which obviously contradicts the anisotropy found in the measurements. A  $\text{Co}^{3+}$  HS system shows the wrong magnetic anisotropy.

Next, we discuss the IS state of  $\text{Co}^{3+}$ . Due to the elongation of the oxygen octahedra, the  $e_g$  electron occupies the  $3z^2 - r^2$  orbital. This also effects the splitting of the  $t_{2g}$  states. The  $xz$  and  $yz$  orbitals remain degenerate but are not degenerate with the  $xy$  orbital. This arises from the different charge distributions in relation to the  $3z^2 - r^2$  orbital. We have five electrons to fill in the  $t_{2g}$  states, which can also be treated as one hole in the  $t_{2g}$  states. This hole is attracted to the  $e_g$  electron in the  $3z^2 - r^2$  orbital. Fig. 4 shows the charge distribution of this hole and the  $3z^2 - r^2$  orbital. In the left sketch, both the electron in the  $3z^2 - r^2$  orbital and a hole in the  $xy$  orbital is drawn. The sketch in the center shows the  $3z^2 - r^2$  orbital and the hole in a linear combination of the degenerate  $xz$  and  $yz$  orbitals. Regarding the distances between the electron and the hole, one can conclude that the state with the hole in the  $xz$  and  $yz$  orbitals is lower in energy. As the order of levels is reversed when we are speaking about holes instead of electrons, this means that the  $xy$  orbital is lowered in energy. Thus, the order and occupation of levels is the one shown in Fig. 4. The magnetic anisotropy is the same as in the case of  $\text{Co}^{3+}$  HS which we treated in the last paragraph. With three electrons in the degenerate level of the  $xz$  and  $yz$  orbitals, we can also make use of Eq. (3) to show that the direction of anisotropy does not fit the measurements for  $\text{La}_{2-x}\text{Sr}_x\text{CoO}_4$ .

Neither the HS nor the IS state of  $\text{Co}^{3+}$  show the correct magnetic anisotropy. But before we draw further conclusions,  $\text{Co}^{2+}$  should be discussed. Although  $\text{Co}^{2+}$  has also been found in the LS state in some intramolecular compounds [21], for bulk crystals it can be safely assumed that  $\text{Co}^{2+}$  is in the HS state [22].

Regarding the ground state produced by the crystal field in Fig. 3, where the lowest level is filled, no linear combinations like in Eq. (3) can be formed. The orbital moment would be completely quenched and the magnetic moment would be determined by an isotropic spin. If, however, spin-orbit coupling is of the same magnitude as the splitting of the  $t_{2g}$  orbitals, it will mix these states. Mixing in a state with orbital moment in the  $z$  direction would require placing a hole in the  $d_{\pm 1}^z$  orbital (see Eq. 3). This would cost an energy equal to the splitting within the  $t_{2g}$  orbitals. It is more favorable to mix in a state with orbital moment in the  $x$  (or  $y$ ) direction by placing a hole in the  $d_{\pm 1}^x$  (or the  $d_{\pm 1}^y$ ) orbital (see Eq. 1). This costs only half of the crystal-field splitting within the  $t_{2g}$  orbitals. An orbital moment in the  $x$  (or  $y$ ) direction costs less energy than in the  $z$  direction. So, the  $xy$  plane will be the easy plane for  $\text{Co}^{2+}$  in this elongated tetragonal structure [24]. The spin moment will also be found in the  $xy$  plane. Comparing these findings to the measurement, we see that  $\text{Co}^{2+}$  shows the correct direction of magnetic

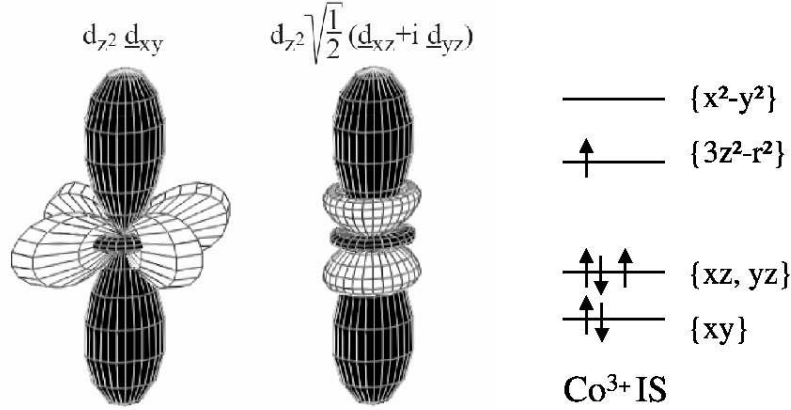


Figure 4: The picture on the left shows the charge distribution for an electron in the  $3z^2 - r^2$  orbital (black) and a hole in the  $xy$  orbital (white). The charge distribution in the center refers to an electron in the  $3z^2 + r^2$  orbital and a hole in a linear combination of the  $xz$  and  $yz$  orbitals. The splitting and the occupation of the 3d levels for  $\text{Co}^{3+}$  in the IS state is shown on the right.

anisotropy. Now a conclusion about the spin state of  $\text{Co}^{3+}$  can be drawn. For  $x \geq 0.5$ , at least half of the cobalt ions in the crystal are  $\text{Co}^{3+}$ . Taking into account that  $\text{Co}^{2+}$  has a smaller spin moment than HS  $\text{Co}^{3+}$ , the latter would dominate the anisotropy. The opposite is, however, the case in the data. Thus, for this doping range, the spin state of  $\text{Co}^{3+}$  is identified with the LS state and the magnetization must be assigned to  $\text{Co}^{2+}$ , which shows the correct anisotropy. For  $x = 0.4$ , we still have 40%  $\text{Co}^{3+}$  and, because of the pronounced anisotropy, we can follow the same argumentation here. Regarding  $x = 0.3$  in Fig. 2, the anisotropy is found to be rather small compared to the other compounds.

It should be stressed that the direction of anisotropy in layered perovskites depends on the direction in which the oxygen octahedron is distorted. In some systems like  $\text{K}_2\text{CoF}_4$  the octahedra are compressed in the  $c$  direction, resulting in an easy-axis anisotropy [23];  $\text{Co}^{2+}$  in almost cubic symmetry also tends to have an easy-axis anisotropy like in  $\text{CoO}$ . However, in our case of  $\text{La}_{2-x}\text{Sr}_x\text{CoO}_4$ , the oxygen octahedron surrounding the cobalt ion is elongated by the inherent tetragonal structure. This situation is comparable to the change of anisotropy in  $\text{CoO}$  films on different substrates [24].

For a quantitative analysis of the data and a confirmation of the results found in the qualitative discussion of the anisotropy, a full-multiplet calculation was carried out within the crystal field approximation [25]. A Hamiltonian for the 3d shell of the  $\text{Co}^{2+}$  ion was set up, including crystal field, spin-orbit coupling and magnetic field. The Slater integrals  $F_0$ ,  $F_2$  and  $F_4$  characterizing the Coulomb interaction and the spin-orbit coupling constant were taken from a Hartree-Fock approximation [20]. Any excitations from the oxygen 2p levels and mixing with higher states were neglected,

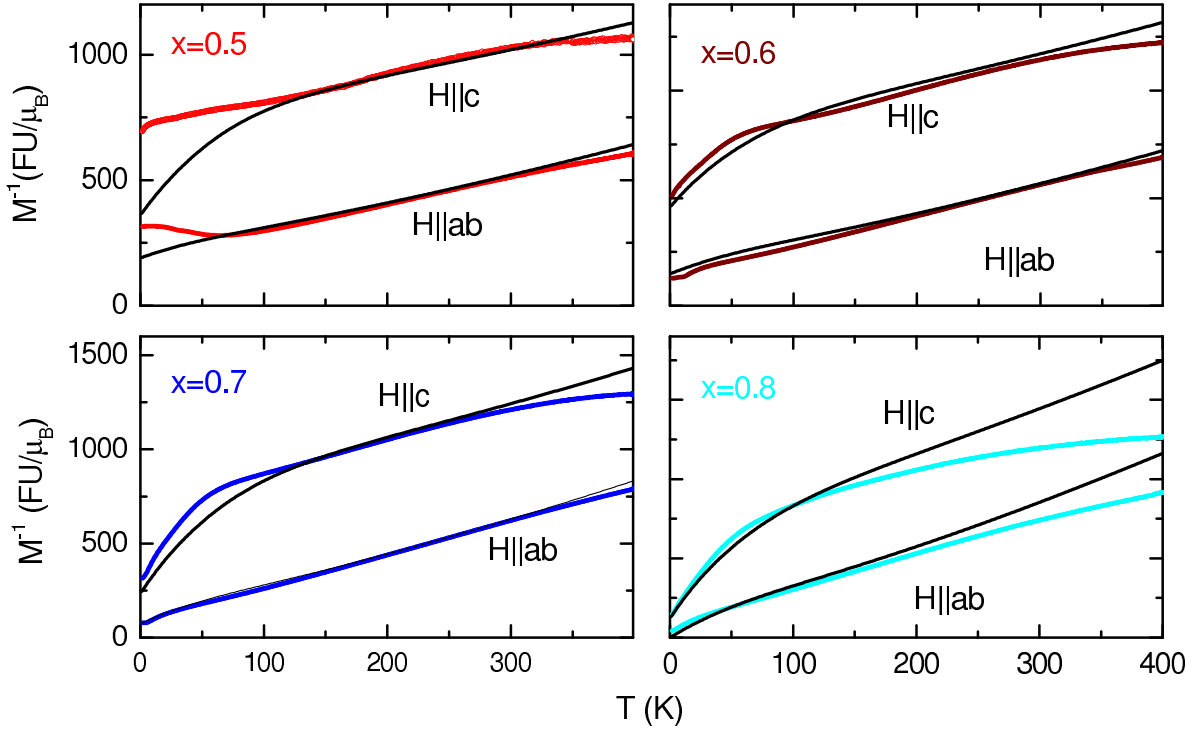


Figure 5: Measured magnetization (colored lines) compared with the calculation for  $Co^{2+}$  (black lines), plotted inverse. A mean-field magnetic exchange was added to the calculation. Note that the magnetization of the ion was weighted with the content of  $Co^{2+}$  ( $1 - x$ ).

as these effects are not significant when considering thermal energies. The parameters for the crystal field were treated semi-empirically. Regarding the tetragonal distortion as a perturbation of the cubic symmetry, the effect of the hybridization of the Co  $3d$  shell with the surrounding oxygen  $2p$  shells only increases the splitting of the cubic  $t_{2g}$  and  $e_g$  states. Hybridization can thus be included into the crystal field parameters and need not be treated separately. The Hamiltonian was diagonalized and Eigenstates and Eigenvalues were used to obtain the temperature dependence of the magnetization. Magnetic exchange was included in the calculation on a mean-field level. The results can be seen in Fig. 5, where the inverse magnetization is plotted.

The crystal-field parameters were chosen as follows: the  $10Dq$  splitting and the splitting within the  $e_g$  levels were fixed at 1.5eV and 0.2eV, respectively. These two values are of minor importance for the calculation, because the anisotropy of the magnetization arises from the  $t_{2g}$  electrons, as described in the discussion above. The splitting of the  $t_{2g}$  states showed up to be crucial for the form and the anisotropy of the calculated curves. The values of the splitting within the  $t_{2g}$  states were chosen as 80meV, 60meV, 68meV, and 50meV for the compounds  $x = 0.5, 0.6, 0.7,$  and  $0.8$ , respectively. These  $t_{2g}$  crystal field splittings for Co are in good agreement with previous measurements on strained CoO thin films [24]. They might appear to be surprisingly small compared to the values found for the Titanates [26, 27] in the order of 200 meV. The difference

between Co and Ti can be understood by considering the radial extent of the  $d$  wave function and the transition metal - oxygen (TM-O) distance. The Co  $d$  wave function is much smaller than the Ti  $d$  wave function, reducing the covalency and thereby the size of the crystal-field splitting. At the same time, the average TM-O distances of  $\text{La}_{2-x}\text{Sr}_x\text{CoO}_4$  and  $\text{LaTiO}_3$  are almost equal ( $\approx 2.02\text{\AA}$  for Co-O [16] and  $\approx 2.04\text{\AA}$  for Ti-O [28]). This is related to the occupation of the anti-bonding  $e_g$  orbitals in a HS  $\text{Co}^{2+}$  compound which pushes the O atoms further away.

It can be seen in Fig. 5 that the calculation gives a good description for  $x = 0.6$  and  $x = 0.7$ . The magnetization of the half-doped sample  $x = 0.5$  is reproduced well for higher temperatures. At temperatures below the freezing temperature, the calculation cannot describe the system because magnetic order is not included in the model. The  $x = 0.8$  sample is fitted well for lower temperatures. Above  $T \approx 350\text{K}$ , the magnetization in the measurement is enhanced by another effect and results in a deviation from the calculation. This effect can be seen in all curves in Fig. 2, but at significantly higher temperatures. This increase of magnetization could arise from the thermal population of the  $\text{Co}^{3+}$  HS or IS state. But surely further measurements at higher temperatures are needed to confirm this assumption. Nevertheless, the full-multiplet calculation of a pure  $\text{Co}^{2+}$  system already succeeds in describing the main features of the magnetization for  $x \geq 0.5$ . This confirms that  $\text{Co}^{3+}$  is a LS system in this doping range.

In summary, the magnetic susceptibility of  $\text{La}_{2-x}\text{Sr}_x\text{CoO}_4$  has been analyzed for two different directions of the external magnetic field. A definite anisotropy of the magnetic moment is found experimentally with  $\chi_{ab} > \chi_c$ . This direction of anisotropy does not match with the behavior of HS or IS  $\text{Co}^{3+}$ , whereas  $\text{Co}^{2+}$  in the HS state shows the correct single-ion anisotropy. Thus, the spin state of  $\text{Co}^{3+}$  for  $x \geq 0.4$  must be the LS state. This conclusion is also confirmed by a full-multiplet calculation.

We acknowledge financial support by the Deutsche Forschungsgemeinschaft through SFB 608.

## References

- [1] Jonker G H, Van Santen J H 1953 *Physica* **XIX**, 120
- [2] Raccah P M, Goodenough J B 1967 *Phys. Rev.* **155**, 932
- [3] Abbate M, Fuggle J C, Fujimori A, Tjeng L H, Chen C T, Potze R, Sawatzky G A, Eisaki H, Uchida S 1993 *Phys. Rev.* **B 47**, 16124
- [4] Korotin M A, Ezhov S Y, Solovyev I V, Anisimov V I, Khomskii D I, Sawatzky G A 1996 *Phys. Rev.* **B 54**, 5309
- [5] Zobel C, Kriener M, Bruns D, Baier J, Grüninger M, Lorenz T, Reutler P, Revcolevschi A 2002 *Phys. Rev.* **B 66**, 020402
- [6] Noguchi S, Kawamata S, Okuda K, Nojiri H, Motokawa M 2002 *Phys. Rev.* **B 66**, 94404
- [7] Maris G, Ren Y, Volotchaev V, Zobel C, Lorenz T, Palstra T T M 2003 *Phys. Rev.* **B 67**, 224423
- [8] Ropka Z, Radwanski R J 2003 *Phys. Rev.* **B 67**, 172401
- [9] Lengsdorf R, Ait-Tahar M, Saxena S S, Ellerby M, Khomskii D I, Micklitz H, Lorenz T, Abd-Elmeguid M M 2004 *Phys. Rev.* **B 69**, 140403
- [10] Baier J, Jodlauk S, Kriener M, Reichl A, Zobel C, Kierspel H, Freimuth A, Lorenz T 2005 *Phys. Rev.* **B 71** 014443

- [11] Haverkort M W, Hu Z, Cezar J C, Burnus T, Hartmann H, Reuther M, Zobel C, Lorenz T, Tanaka A, Brookes N B, Hsieh H H, Lin H J, Chen C T, Tjeng L H 2006 Phys. Rev. Lett. **97** 176405
- [12] Moritomo Y, Higashi K, Matsuda K, Nakamura A 1997 Phys. Rev. **B 55** R14725
- [13] Itoh M, Mori M, Moritomo Y, Nakamura A 1999 Physica **B 259-261** 997-998
- [14] Wang J, Tao Y C, Zhang W, Xing D Y 2000 J. Phys.: Condensed Matter **12**, 7425-7432
- [15] Zaliznyak I A, Hill J P, Tranquada J M, Erwin R, Moritomo Y 2000 Phys. Rev. Lett. **85** 4353
- [16] Cwik M 2007 PhD thesis, University of Cologne
- [17] Bruno P 1989 Phys. Rev. **B 39** 865
- [18] Goodenough J B 1968 Phys. Rev. **171** 466
- [19] Kamimura H 1956 J. Phys. Soc. Japan **11** 1171
- [20] Haverkort M W 2004 PhD thesis, University of Cologne
- [21] Brooker S, de Geest D J, Kelly R J, Plieger P G, Moubaraki B, Murray K S, Jameson G B 2002 J. Chem. Soc., Dalton Trans., 2080 - 2087
- [22] Goodenough J B, *Magnetism and the Chemical Bond* 1963 Wiley
- [23] Folen V J, Krebs J J, Rubinstein M 1968 Solid State Comm. **6** 865
- [24] Csiszar S I, Haverkort M W, Hu Z, Tanaka A, Hsieh H H, Lin H J, Chen C T, Hibma T, Tjeng L H 2005 Phys. Rev. Lett. **95**, 187205
- [25] Here we refer to standard textbooks like Ballhausen C J, *Introduction to Ligand Field Theory* 1962 McGraw-Hill; Sugano S, Tanabe Y, Kamimura H, *Multiplets of Transition-Metal Ions in Crystals* 1972 Academic Press
- [26] Haverkort M W, Hu Z, Tanaka A, Ghiringhelli G, Roth H, Cwik M, Lorenz T, Schüßler-Langeheine C, Streltsov S V, Mylnikova A S, Anisimov V I, De Nadai C, Brookes N B, Hsieh H H, Lin H J, Chen C T, Mizokawa T, Taguchi Y, Tokura Y, Khomskii D I, Tjeng L H 2005 Phys. Rev. Lett. **94** 056401
- [27] Rückamp R, Benckiser E, Haverkort M W, Roth H, Lorenz T, Freimuth A, Jongen L, Möller A, Meyer G, Reutler P, Büchner B, Revcolevschi A, Cheong S W, Sekar C, Krabbes G, Grüninger M 2005 New Journal of Physics **7** 144
- [28] Cwik M, Lorenz T, Baier J, Müller R, André G, Bourée F, Lichtenberg F, Freimuth A, Schmitz R, Müller-Hartmann E, Braden M 2003 Phys. Rev. **B 68**, 060401(R)